

BISTATIC RADAR OBSERVATIONS OF THE MOON USING MINI-RF ON LRO AND THE ARECIBO OBSERVATORY. G.W. Patterson, D.B.J. Bussey, and the Mini-RF Team. Johns Hopkins University Applied Physics Laboratory, Laurel, MD (Wes.Patterson@jhuapl.edu).

Introduction: The Mini-RF team is acquiring bistatic radar measurements of the lunar surface to understand the scattering properties of materials as a function of phase angle. These observations have produced the first lunar bistatic radar images ever collected with non-zero phase angles. The goal of these observations is to differentiate between scattering indicative of surfaces that are rough versus surfaces that harbor water ice in quantities detectable by a radar system operating at a wavelength of 12.6 cm.

Bistatic Operations: Radar observations of planetary surfaces provide unique information on the structure (i.e., roughness) and dielectric properties of surface and buried materials [e.g., 1-4]. These data can be acquired using a monostatic architecture, where a single antenna serves as the signal transmitter and receiver, or they can be acquired using a bistatic architecture, where a signal is transmitted from one location and received at another. The former provides information on the scattering properties of a target surface at zero phase. The latter provides the same information over a variety of phase angles. NASA's Mini-RF instrument on the Lunar Reconnaissance Orbiter and the Arecibo Observatory in Puerto Rico are currently operating in a bistatic architecture (the Arecibo Observatory serves as the transmitter and Mini-RF serves as the receiver). This architecture maintains the hybrid dual-polarimetric nature of the Mini-RF instrument [5] and, therefore, allows for the calculation of the Stokes parameters (S_1 , S_2 , S_3 , S_4) that characterize the backscattered signal (and the products derived from those parameters).

Observations: A common product derived from the Stokes parameters is the Circular Polarization Ratio (CPR),

$$\mu_C = \frac{(S_1 - S_4)}{(S_1 + S_4)} \quad (1).$$

High CPR values can serve as an indicator of rough surfaces [4,5] or as an indicator of the presence of water ice [6]. Recent work using monostatic radar data and inferences from surface geology suggests that anomalously high CPR values associated with some polar lunar craters are indicative of the presence of water ice [7,8]. However, a unique determination of water ice is hindered by the surface roughness characteristics of craters [4]. Bistatic radar data can take advantage of differences in the CPR characteristics of rough surfaces and water ice as a function of phase

angle to differentiate between these possibilities [9-11]. To do so, Mini-RF is currently acquiring bistatic radar data of lunar polar and non-polar crater materials.

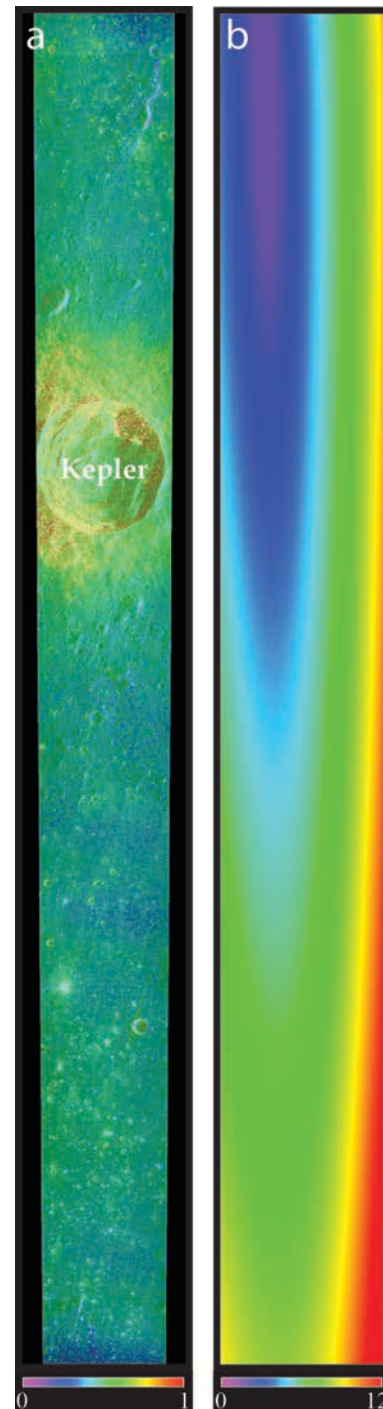


Fig. 1. Bistatic (a) CPR and (b) phase angle information for Kepler crater (8.1°N, 38.0°W, dia. 32 km).

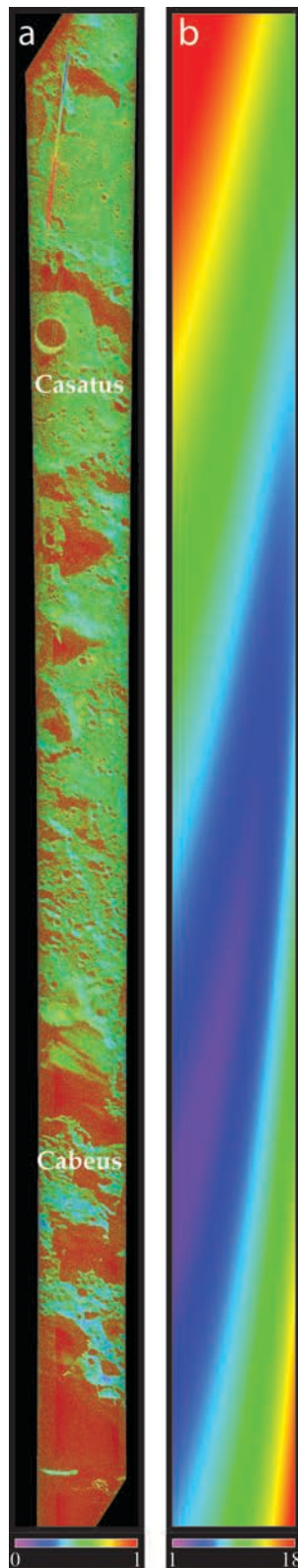


Fig. 2. Bistatic (a) CPR and (b) phase angle information for Casatus (72.6°S, 30.5°W, dia. 111 km) and Cabeus craters (84.9°S, 35.5°W, dia. 98 km).

To characterize the CPR of solely rough surfaces as a function of phase angle, we are acquiring bistatic radar data of a number of relatively fresh non-polar craters that have high monostatic CPR values (e.g., Fig. 1). This information can then be compared directly to data acquired of polar targets that include anomalous craters identified by [7,8] (e.g., Fig. 2).

Results: Initial analysis shows that the CPR of mare materials are only weakly sensitive to variations in phase angle and that the CPR of crater ejecta increases steadily for phase angles $< 5^\circ$. This is markedly different from the expected behavior of water ice [9]. Bistatic data for polar craters clearly indicate the presence of crater material associated with small fresh impacts (yellow – Fig. 2). Analysis of the phase angle characteristics of these materials and polar crater floors is ongoing.

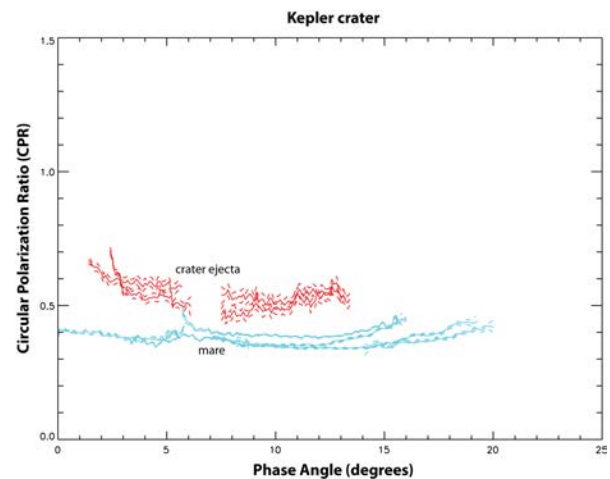


Fig. 3. Plot of CPR vs. phase angle for crater ejecta and mare materials associated with Kepler crater (Fig. 2).

References: [1] Campbell et al. (2010), *Icarus*, 208, 565-573; [2] Raney et al. (2012), *JGR*, 117, E00H21; [3] Carter et al. (2012), *JGR*, 117, E00H09; [4] Campbell (2012), *JGR*, 117, E06008; [5] Raney, R. K. et al. (2011), *Proc. of the IEEE*, 99, 808-823; [6] Black et al. (2001), *Icarus*, 151, 167-180; [7] Spudis et al. (2010), *GRL*, 37, L06204; [8] Spudis et al. (2013), *JGR*, in review; [9] Hapke and Blewett (1991), *Nature*, 352, 46-47; [10] Nelson et al. (2000), *Icarus*, 147, 545-558; [11] Piatek et al. (2004), *Icarus*, 171, 531-545.